



On the Benefits of Using Gyroscope Measurements with Structure from Motion

Adel Fakih, John Zelek

► To cite this version:

Adel Fakih, John Zelek. On the Benefits of Using Gyroscope Measurements with Structure from Motion. Workshop on Multi-camera and Multi-modal Sensor Fusion Algorithms and Applications - M2SFA2 2008, Andrea Cavallaro and Hamid Aghajan, Oct 2008, Marseille, France. inria-00326771

HAL Id: inria-00326771

<https://inria.hal.science/inria-00326771>

Submitted on 5 Oct 2008

HAL is a multi-disciplinary open access archive for the deposit and dissemination of scientific research documents, whether they are published or not. The documents may come from teaching and research institutions in France or abroad, or from public or private research centers.

L'archive ouverte pluridisciplinaire **HAL**, est destinée au dépôt et à la diffusion de documents scientifiques de niveau recherche, publiés ou non, émanant des établissements d'enseignement et de recherche français ou étrangers, des laboratoires publics ou privés.

On the Benefits of Using Gyroscope Measurements with Structure from Motion

Adel Fakh and John Zelek

University of Waterloo

Abstract. This paper is concerned with the benefits of using rotational measurements of a gyroscope in conjunction with optical flow to determine the instantaneous rigid motion. It presents an experimental study focusing on three main aspects: speedup, resolving ambiguities due to local minima and accuracy. For this sake, we developed a method to minimize simultaneously the reprojected optical flow error and the deviation from the gyro measurements, in line with the optimal Structure from Motion techniques. We show that the gyro measurements can be used in a procedure to initialize the iterative estimation which results in a considerable speedup. We show also that minimizing both the deviation from the measured flow and the gyro measurements gives better results for the rotational velocity when the gyro measurements are not very noisy. It doesn't affect the accuracy of the translational velocity, however if the gyro measurements are very noisy it might lead to erroneous translational estimates.

1 Introduction

The instantaneous estimation of the motion of a rigid body is essential to many robotics applications. Towards this aim, some researches [3, 9, 14–16] have proposed using both vision and Inertial measurements to estimate the instantaneous motion. The premise is to exploit the complementary properties of the two sensors and to compensate their respective weaknesses.

In this paper we focus on the rotational rate reading of a gyroscope and the benefits that can be obtained from using these measurements with optical flow to determine the ego-motion. We are interested in the required computation time, resolving ambiguities and the accuracy of the estimates. Specifically we are interested in how the gyro measurements might affect the translational estimates. Some published results [5, 16] suggest that the rate measurements improve the accuracy of the translational estimates. However, this has not been thoroughly addressed and the experiments presented were not extensive enough on this point to help form a decisive opinion.

In contrast to previous works that used the rate measurements within a recursive filter [5, 16] which might obscure the way they affect the estimates, we propose to use a single optical flow field and find the estimates that minimize simultaneously the distance between the reprojected optical flow error and the deviation from the gyro measurements. We developed a method to do this as an extension to the iterative optimal Structure From Motion (SFM) techniques [4, 13, 17] introduced recently (optimal is

defined as leading to unbiased estimates with minimal variance of the estimates). Also we present a procedure to determine reliable initial estimates for the iterations using the gyro measurements in such a way to avoid falling in local minima.

The findings of our experiments are that using the gyro measurements for initialization can significantly decrease the running time. For the rotational estimates, when the gyro measurement is more accurate than the vision estimate, the estimate combining both vision and gyro is better than vision and worse than gyro. When the gyro measurement is worse than vision the estimate combining both is as good as vision. Since in real life, gyro measurements are very noisy, fluctuate a lot and are not as stable as vision, the combination of both is better or at least as good as either one. However the gyro measurements do not affect the accuracy of the translational estimates. Though they help correct some erroneous translational motion in some cases, they introduce new erroneous translations in other cases.

The remainder of this paper is as follows: In section 2 we explain the basics of the problem. Section 3 provides the method used to incorporate the gyro measurements with optical flow and the procedure used to initialize the iterations from the gyro measurements. Section 4 provides experimental results on simulated and real data and Section 5 is a conclusion.

2 Preliminaries

Assuming a perspective projection model, the projection of a 3-D point $\vec{X} = (X, Y, Z)^T$ on the image plane of a camera located in the origin and facing the Z axis is:

$$\vec{x} = \begin{bmatrix} x \\ y \end{bmatrix} = \begin{bmatrix} f \frac{X}{Z} \\ f \frac{Y}{Z} \end{bmatrix}. \quad (1)$$

f is the focal “length” taken wlog as 1. A calibrated Euclidean framework is assumed. If the camera moves with a translational velocity $\vec{V} = (V_x, V_y, V_z)^T$ and a rotational velocity $\vec{\omega} = (\omega_x, \omega_y, \omega_z)^T$, the motion of \vec{X} with respect to the camera will be:

$$\left(\frac{dX}{dt}, \frac{dY}{dt}, \frac{dZ}{dt} \right)^T = -(\vec{\omega} \times \vec{X} + \vec{V}). \quad (2)$$

Substituting the time derivatives of Eq 1 in Eq 2:

$$\dot{\vec{x}}(\vec{x}) = -\frac{A(\vec{x})\vec{V}}{Z} - B(\vec{x})\vec{\omega}, \quad (3)$$

where

$$A(\vec{x}) = \begin{bmatrix} 1 & 0 & -x \\ 0 & 1 & -y \end{bmatrix} \text{ and } B(\vec{x}) = \begin{bmatrix} -xy & 1+x^2 & -y \\ -1-y^2 & xy & x \end{bmatrix}. \quad (4)$$

$\dot{\vec{x}}$ is the image velocity (optical flow) at the pixel \vec{x} and can be considered as the sum of three components, a translational component $\dot{\vec{x}}_V = \frac{A(\vec{x})\vec{V}}{Z}$, a rotational component $\dot{\vec{x}}_\omega = B(\vec{x})\vec{\omega}$ and an independently and identically distributed Gaussian noise term

$n(\vec{x})$. Figure 1 illustrates these components along with the unit vector $\vec{\tau}(\vec{x}, \vec{V}, 1)$ [17], orthogonal to the translational flow:

$$\vec{\tau}(\vec{x}, \vec{V}, 1) = \frac{1}{\|A(\vec{x})\vec{V}\|} ([A(\vec{x})\vec{V}]_y, -[A(\vec{x})\vec{V}]_x)^T, \quad (5)$$

where $[A(\vec{x})\vec{V}]_x$ and $[A(\vec{x})\vec{V}]_y$ refer to the x and y components of the vector $A(\vec{x})\vec{V}$ respectively. Non optimal techniques [6–8, 10–12] eliminate the depth from Eq.3 and

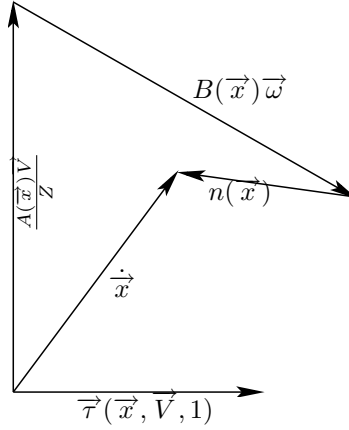


Fig. 1. Components of optical flow.

reach to the bilinear constraint [2]:

$$\|A(\vec{x})\vec{V}\| \vec{\tau}(\vec{x}, \vec{V}, 1)^T (\dot{\vec{x}} - B(\vec{x})\vec{\omega}) = 0. \quad (6)$$

Then they determine the 3D parameters that minimize this equation. This is exactly what makes them non-optimal because Figure 1 shows that the true constraint is:

$$\vec{\tau}(\vec{x}, \vec{V}, 1)^T (\dot{\vec{x}} - B(\vec{x})\vec{\omega}) = 0, \quad (7)$$

which is the projection of the constraint in Equation 3 on the direction of $\vec{\tau}$. Therefore the constraint in Equation 6 is incorrect because it weights the true constraint by $\|A(\vec{x})\vec{V}\|$ which is different for different points \vec{x} . Optimal algorithms [4, 13, 17] determine the motion and the depth simultaneously by minimizing the unweighted constraint (Equation 7). The unweighted constraint have an error surface much more complex than the weighted one which makes its minimization much more challenging.

An analysis of Figure 1 shows that even if the rotational velocity $\vec{\omega}$ is perfectly known, this won't necessarily lead to a more accurate translational estimate. In the next Section we develop an algorithm to minimize simultaneously the deviation from the measured optical flow and from the gyro measurements. The experimental results we obtain are in accord with the aforementioned claim.

3 Extending Optimal Techniques to Minimize the Flow Reprojection Error and the Deviation from the Gyro

Assume that N optical flow values $\dot{\vec{x}}_i, i = 0, \dots, N - 1$ are available along with the corresponding readings $\vec{\omega}_g = (\omega_{gx}, \omega_{gy}, \omega_{gz})^T$ of a gyroscope. We use $d(\vec{x})$ to represent the inverse depth corresponding to the point \vec{x} and \vec{d} to represent the vector of inverse depths of the all N points.

The starting point is to define a residual vector between the reprojected flow of the estimates and the measurements. For this aim we define the gyro flow $\dot{\vec{x}}_g$ as the image velocities projected by $\vec{\omega}_g$ at each of the N points.

$$\dot{\vec{x}}_g = B(\vec{x})\vec{\omega}_g. \quad (8)$$

We formulate the residual function accounting for both optical flow and gyro measurements as:

$$\vec{r}(\vec{x}) = \alpha(\vec{x}(\vec{x}) - \frac{A(\vec{x})\vec{V}}{Z} - B(\vec{x})\vec{\omega}) + \beta(B(\vec{x})\vec{\omega}_g - B(\vec{x})\vec{\omega}). \quad (9)$$

The parameters α and β depend on the noise distribution in the measured optical flow and the gyro flow. α and β should be proportional to σ_g and σ_v respectively, where σ_g is the standard deviation of the noise in the gyro flow and σ_v is the standard deviation of the noise in the image estimated optical flow. To eliminate the depth we multiply by the vector $\vec{\tau}(\vec{x})$ and obtain \vec{r}_τ , the component of \vec{r} in the direction of $\vec{\tau}$:

$$\vec{r}_e(\vec{x}) = \vec{\tau}(\vec{x}, \vec{V}, 1)^T (\alpha \vec{x} + \beta B(\vec{x})\vec{\omega}_g - (\alpha + \beta)B(\vec{x})\vec{\omega}) \quad (10)$$

The optimal estimator is defined as

$$(\hat{\vec{\theta}}) = \underset{\vec{\theta}}{\operatorname{argmin}} \frac{1}{N} \sum_{\vec{x}} \|\vec{r}(\vec{x})\|, \quad (11)$$

where $\vec{\theta} = [\vec{V}^T, \vec{\omega}^T, \vec{d}^T]^T$ is the vector of the unknown 3D parameters. The absolute values of \vec{V} and \vec{d} cannot be determined therefore we fix the magnitude of \vec{V} to 1. Starting from this formulation we develop a numerical algorithm to get the 3D estimates. The algorithm is an iterative Gauss-Newton procedure having the following linear system at the basic iteration k :

$$J_k \Delta \theta_k = -\vec{r}_k, \quad (12)$$

where $\vec{r}_k = [\vec{r}_1^T, \dots, \vec{r}_N^T]^T$ and J_k is the Jacobian of \vec{r}_k . Each equation of this linear system has the following form:

$$\alpha[d_k(\vec{x})A(\vec{x})\Delta\vec{V}_k + A(\vec{x})\vec{V}_k\Delta d_k(\vec{x})] + (\alpha + \beta)B(\vec{x})\Delta\vec{\omega}_k = \vec{r}_k(\vec{x}) \quad (13)$$

The constraint ($\|\vec{V}\| = 1$) leads to the additional linear equation: ($\vec{V}_k^T \Delta\vec{V}_k = 0$).

Then as in [17] we use the separability of $\vec{\theta}$ as $\vec{\theta} = (\vec{V}, (\vec{\omega}, \vec{d}))$ in the sense that if \vec{V} is known, then $(\vec{\omega}$ and $\vec{d})$ can be determined by solving a linear problem. After each Gauss-Newton iteration we use only $\Delta\vec{V}_k$ to get \vec{V}_{k+1} and determine $\vec{\omega} + \vec{1}$ using equation 10 which when \vec{V} is known, leads to a linear least squares equation in $\vec{\omega}$. After $\vec{\omega}_{k+1}$ is determined \vec{d}_{k+1} can be determined as follows:

$$d_{k+1}(\vec{x}) = \frac{[A(\vec{x})\vec{V}_{k+1}]^T \left((\alpha + \beta)B(\vec{x})\vec{\omega}_{k+1} - \dot{\vec{x}} - \beta B(\vec{x})\vec{\omega}_g \right)}{\|A(\vec{x})\vec{V}_{k+1}\|^2} \quad (14)$$

3.1 Initializing the iterations using the gyro measurements

The initialization of the iterations is a problem for optimal techniques because the chances of falling in a local minimum depend directly on the initial values. Zhang and Tomasi [17] solve this by starting from 15 different initializations spread on the unit hemisphere for \vec{V} , which results in a longer execution time. Pauwels and Van hulle [13] proposed a method that starts from the weighted constraint Eq. 6 (as in non-optimal approaches) and gradually unweights it through the Gauss-Newton iterations. This way it can be initialized from any point and avoids many of the local minima however it takes more time to converge. We show here that the gyro measurements can be used to provide a good initialization of the iterations avoiding many of the local minima. We set $\vec{\omega}_0 = \vec{\omega}_g$. Then we undo the rotation of $\vec{\omega}_0$ by subtracting $B(\vec{x})\vec{\omega}_0$ from the measured optical flow. The residual flow is supposed to be just translational and the translational velocity corresponding can be recovered in a closed form. For a translational flow field, equation 10 gives \vec{V}_{k+1} as:

$$\vec{V}_{k+1} = \underset{\vec{V}}{\operatorname{argmin}} \sum [\tau(\vec{x}, \vec{V}, 1)^T \vec{x}]^2. \quad (15)$$

\vec{V} can then be determined as the null space of the matrix

$$M = \sum (\vec{E}\vec{E}'), \quad (16)$$

where $\vec{E} = (-\dot{y}, \dot{x}, \dot{y}x - \dot{x}y)^T$. The solution is the eigenvector of M corresponding to the smallest eigen value. However, due to noise all the eigen values of E might be close to each others. Then each one of the eigen vectors corresponds to a local minimum, and the true solution might not be the one corresponding to the smallest eigen value. Therefore, the three eigen vectors of E should be taken into consideration. Actually, those minima correspond to the bas-relief ambiguity [1]. We resolve this ambiguity by initializing from three different places-each one corresponding to one of the eigen vectors of E -and choosing the final estimate which corresponds to the minimum reprojection error.

4 Experimental Results

4.1 Simulation results

Random clouds of 70 points are generated in a depth range of 2 – 8 focal lengths. The focal length is set to 1 and the focal plane dimensions to 2×2 focal lengths. The field of view is set to 80° . We generate simulation translational and rotational velocities as follows:

$$\begin{aligned}\vec{V} &= [\sim \mathcal{N}(0, 0.5) \sim \mathcal{N}(0, 0.5) \sim \mathcal{N}(0, 0.5)] \\ \vec{\omega} &= [\sim \mathcal{N}(0, 0.02) \sim \mathcal{N}(0, 0.02) \sim \mathcal{N}(0, 0.02)];\end{aligned}\tag{17}$$

where $\sim \mathcal{N}(0, \sigma)$ refers to a sample drawn from a zero mean Gaussian distribution with standard deviation σ . The magnitudes of the resulting rotational flow and translational flow are close to each other. Gaussian noise with different standard deviations in different runs is added to the optical flow field. To model the gyro measurements we add Gaussian noise to the true rotational velocity and use it as the gyro measurements. To compare the estimates against vision only estimates we use the optimal method of Zhang and Tomasi [17].

In the first set of experiments we aim to evaluate the effect of using the gyro data to initialize the iterations as in section 3.1. We performed an extensive number of runs with different noise levels in the optical flow and in the gyro measurements. The parameter β is set to zero which means that the gyro data is just used for initialization and not in the estimation process. Our findings on this point show that the initialization using the 3 initial estimates provided by the gyro data lead always to the same convergence as Zhang and Tomasi which needs to be initialized from 15 different initial estimates evenly spread to guarantee convergence to the global minimum. This results in a speedup of almost 5 times. Figure 2 shows the results for $\mathcal{N}(0, 0.008)$ noise in the gyro measurements (up to 40%). The rotational velocity and translational velocity errors are the same as in Zhang and Tomasi, however with much less computational time.

In the second set of experiments we focus on the role of the gyro measurements during the iterative minimization procedure (i.e, using the method developed in Section 3). We start by studying the effect of a noise-free gyro measurement during the minimization. We set β to 0.5. As shown in Figure 3 the rotational velocity estimate accuracy is much better than Zhang and Tomasi. As we are using the correct rotational velocity, one might expect that the translational estimates should be better than the ones recovered from the optical flow only. However, we found always that the translational velocity accuracy is almost the same. This leads to the conclusion that the rotational measurement does not help in improving the accuracy of the translational estimates.

To study the effect of noisy gyro data we performed many experiments with different noise levels in the gyro data and different values of the parameter β . The conclusion is that when the gyro measurements are more accurate than the vision estimate, the resulting rotational velocity is more accurate than the vision only estimate. Increasing the noise in the gyro measurement will increase the noise in the estimates, but overall the error in the estimates does not exceed the error in the vision only estimates even when the gyro measurements are less accurate than the vision estimates. Figure 4 corresponds to results with $\mathcal{N}(0, 0.004)$ noise in the gyro estimates and a β of 0.2.

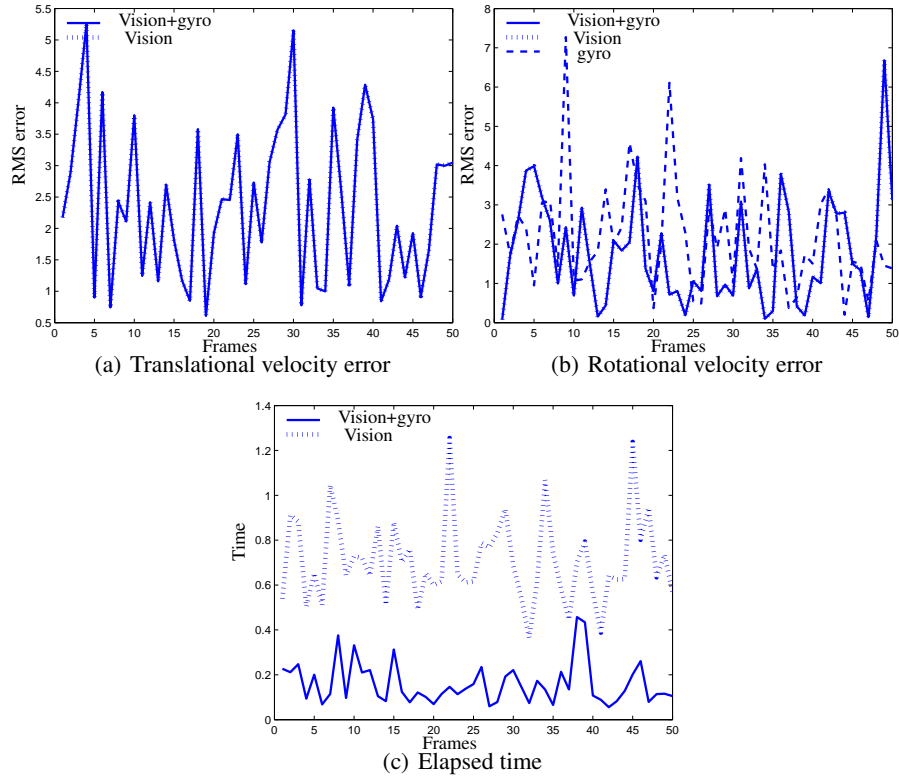


Fig. 2. Initializing using noisy gyro measurements. The initialization is very efficient and achieves the same results as Zhang and Tomasi with much less time.

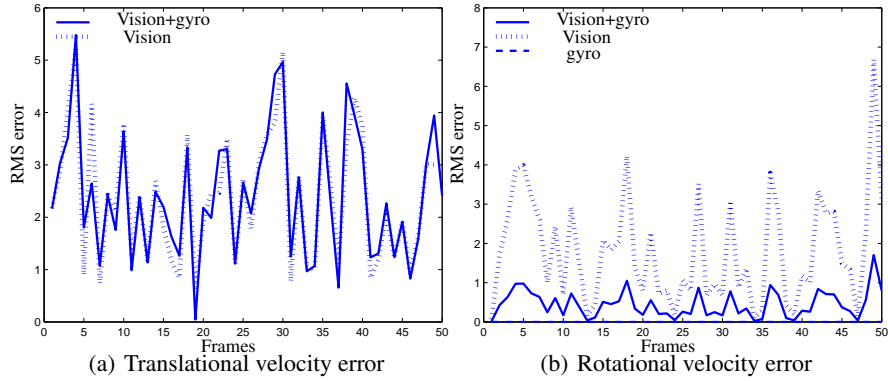


Fig. 3. Using the correct rotational velocity in the minimization ($\beta = 0.5$). The rotational velocity accuracy is better than vision. The translational estimate is minimally affected.

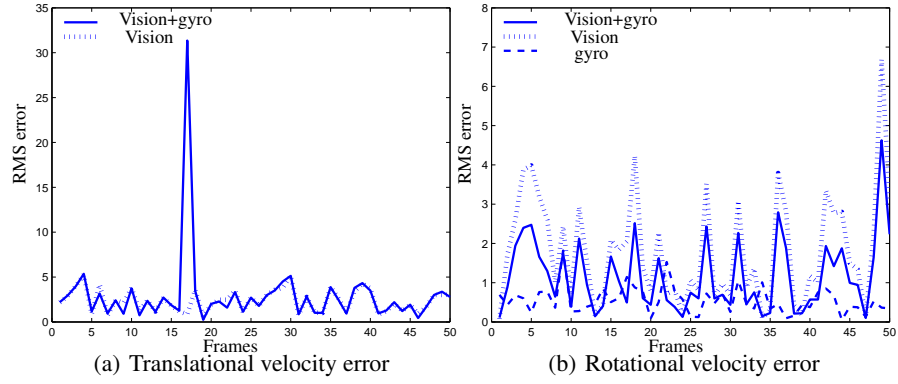


Fig. 4. Using noisy rotational velocity in the minimization ($\beta = 0.2$). The rotational estimate is better than vision if the gyro measurement is better than vision.

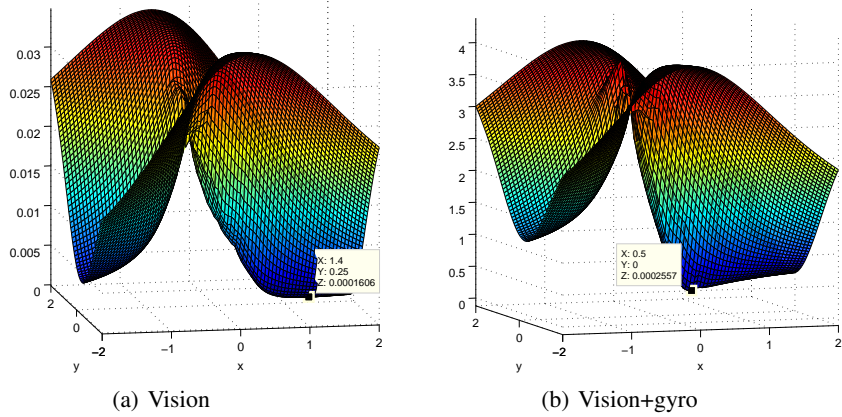


Fig. 5. Reprojection error surfaces with corresponding minima. The minimum of the surface with gyro data is far away from the true minimum. The correct minimum should be at (1.4249, 0.2806).

An interesting phenomenon that happens frequently is shown in frame 17 of Figure 4-a. The translational estimate with gyro for this frame is totally wrong. The reason for this is that the simultaneous minimization of the optical flow reprojection error and the deviation from the gyro measurements introduces a change in the error function surface. This change depends on the distribution of the feature points and the direction of motion. In most of the cases the change does not alter the position of the minimum. However in some other cases the change might be so severe so that a wrong minimum might be smaller than the true one. Figure 5 illustrates that effect for the mentioned frame 17. The true translational heading direction is $(1.4249, 0.2806, 1.0000)$, while the minimum of the error surface when the gyro data is involved happens to be at $(0.5, 0, 1)$. The phenomenon might happen the other-way round also meaning that the change in the error surface might be corrective in such a way that it brings a wrong minimum back to be greater than the true minimum.

4.2 Real Images

In this case we present some results on real data sets. For this purpose a setup comprising a pan-tilt unit (PTU), a camera and an inertial sensor (Figure 6) has been built. The stereo camera is used because the manufacturer provides the intrinsic calibration parameters so we spare the burden of calibration. The motion of the PTU is used as a ground truth. Figure 7 shows a frame from an indoor sequence with the optical flow computed

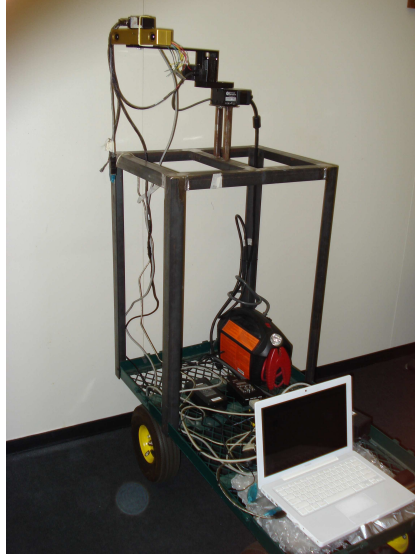


Fig. 6. Setup used to get real data.

for this frame. Shown also in the same figure is the running time taken by Zhang and Tomasi's method and the running time with gyro measurements. Again we see that the

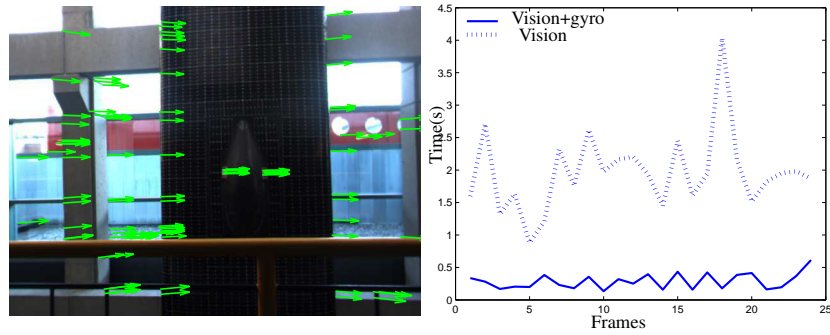


Fig. 7. Optical flow of a frame from an indoor data set and the time required to compute the 3D parameters for the set.

initialization using the gyro gives almost a 5 times speedup. Figure 8 shows the results

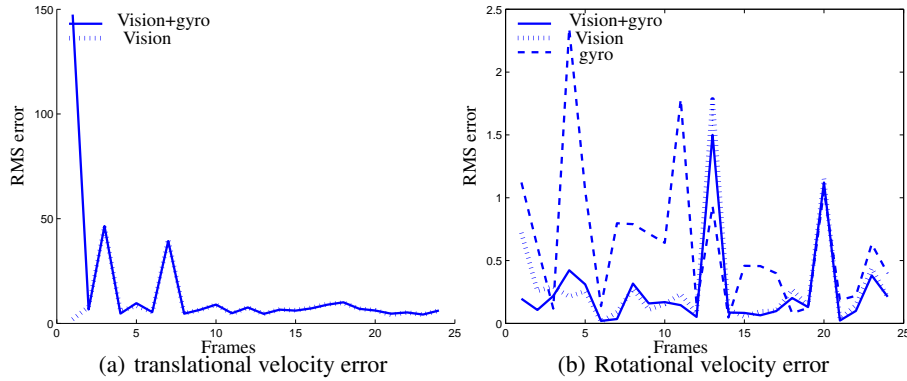


Fig. 8. Results on an indoor sequence.

obtained for 22 frames of this sequence. The same conclusions drawn for simulation data still apply for this case. Figure 9 shows two frames from two outdoor sequences with the corresponding optical flow fields. Figures 10 and 11 show the results of the two outdoor sequences. For these sequences we can see that the incorporation of the gyro data helped in some frames to correct some of the erroneous estimates, however it introduced new erroneous estimates in other cases. For the rotational estimates, as we mentioned before, although the gyro measurements are worse than the vision estimates, the combination of the two is always the same or even better than the estimate of vision alone.



Fig. 9. Optical flow of a 2 frames from the 2 outdoor sequences.

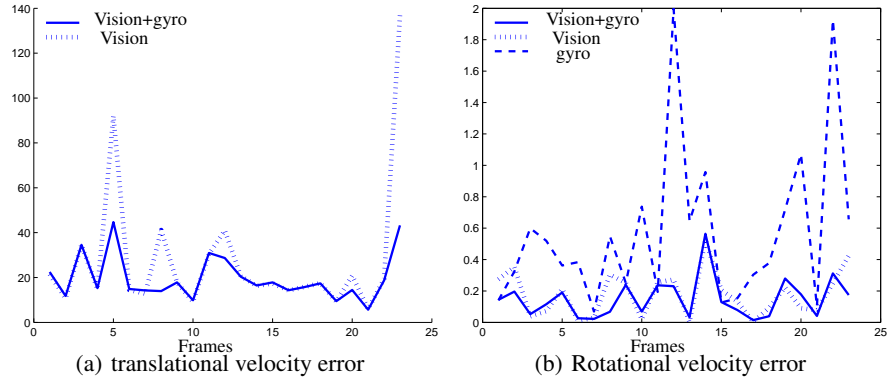


Fig. 10. Results on an outdoor sequence.

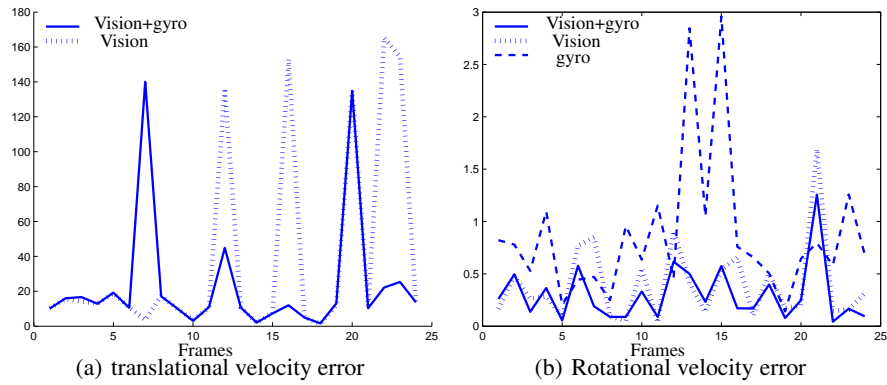


Fig. 11. Results on another outdoor sequence sequence.

5 Conclusion

This paper studied the incorporation of gyro measurements in the ego-motion estimation from a single optical flow field. We showed that the gyro measurements could be used to initialize the iterations which results in about 5 times speedup. We showed also that the simultaneous minimization of both the deviation from the gyro measurements and the reprojected optical flow though it helps in getting better rotational velocity estimates does not result in any significant improvements of the translational estimates. Our results suggest that it would be better to use the gyro just for initialization. After that, a better approach to use the gyro measurements in the estimation would be to compute the translational and rotational velocities from optical flow alone, then in a next step a Kalman like filter can be setup to fuse the rotational velocity only (without any involvement of the translational velocity) with the gyro measurement.

References

1. P. Belhumeur, D. Kriegman, and A. Yuille. The bas-relief ambiguity. *International Journal of Computer Vision*, 35(1):33–44, 1999.
2. A. Bruss and B. Horn. Passive navigation. *Computer Vision, Graphics, and Image Processing*, 21:3–20, 1983.
3. M. CHIKUMA, Z. HU, and K. UCHIMURA. Fusion of Vision, GPS and 3D-Gyro in Solving Camera Global Registration Problem for Vision-based Road Navigation. *IEIC Technical Report (Institute of Electronics, Information and Communication Engineers)*, 103(643):71–76, 2004.
4. A. Chiuso, R. Brockett, and S. Soatto. Optimal structure from motion: Local ambiguities and global estimates. *International Journal of Computer Vision*, 39(3):195–228, 2000.
5. G. Qian and R. Chellappa. Structure from motion using sequential monte carlo methods. *International Journal of Computer Vision*, 59(1):5–31, 2004.
6. D. Heeger and A. D. Jepson. Subspace methods for recovering rigid motion i: Algorithm and implementation. *International Journal of Computer Vision*, 7(2):95–117, January, 1992.
7. A. Jepson and D. Heeger. Linear subspace methods for recovering rigid motion. *Spatial Vision in Humans and Robots*, Cambridge University Press, 1992.
8. A. Jepson and D. Heeger. Linear subspace methods for recovering translational direction. U. of Toronto TR RBCV-TR-92-40, 1992, p. 19, 1992.
9. E. Jones, A. Vedaldi, and S. Soatto. Inertial structure from motion with autocalibration. In *Proceedings of the ICCV Workshop on Dynamical Vision*, 2007.
10. K. Kanatani. Renormalization for unbiased estimation. *ICCV*, 93:599–606, 1993.
11. W. MacLean, A. Jepson, and R. Frecker. Recovery of egomotion and segmentation of independent object motion using the em algorithm. In *5th British Machine Vision Conference, York*, pages 175–184, 1994.
12. W. J. MacLean. Removal of translation bias when using subspace methods. *Computer Vision, 1999. The Proceedings of the Seventh IEEE International Conference on*, 2:753–758, 1999.
13. K. Pauwels and M. M. van Hulle. Optimal instantaneous rigid motion estimation insensitive to local minima. *Comput. Vis. Image Underst.*, 104(1):77–86, 2006.
14. G. Qian, R. Chellappa, and Q. Zheng. Robust structure from motion estimation using inertial data. *Journal of the Optical Society of America A*, 18:2982–2997, 2001.
15. S. Singh and K. Waldron. Motion Estimation by Optical Flow and Inertial Measurements for Dynamic Legged Locomotion. *IEEE Conference on Robotics and Automation*, 2005.
16. S. You and U. Neumann. Fusion of vision and gyro tracking for robust augmented reality registration. *Proc. IEEE Conference on Virtual Reality*, pages 71–78, 2001.
17. T. Zhang and C. Tomasi. On the consistency of instantaneous rigid motion estimation. *Int. J. Comput. Vision*, 46(1):51–79, 2002.